

1 **Title: TNF-mediated survival of CD169⁺ cells promotes immune activation during**
2 **vesicular stomatitis virus infection**

3 Prashant V. Shinde^{1,2}, Haifeng C. Xu^{1,2}, Sathish Kumar Maney^{1,2}, Andreas Kloetgen^{3,4}, Sukumar Namineni^{5,13},
4 Yuan Zhuang^{1,2}, Nadine Honke⁶, Namir Shaabani⁷, Nicolas Bellora⁸, Mareike Doerrenberg³, Mirko Trilling⁹,
5 Vitaly I. Pozdeev^{1,2}, Nico van Rooijen¹⁰, Stefanie Scheu¹¹, Klaus Pfeffer¹¹, Paul R. Crocker¹², Masato Tanaka¹³
6 Sujitha Duggimpudi³, Percy Knolle¹⁴, Mathias Heikenwalder^{5,15}, Jürgen Ruland¹⁶, Tak W. Mak¹⁷, Dirk
7 Brenner^{18,19}, Aleksandra A. Pandya⁶, Jessica I. Hoell³, Arndt Borkhardt³, Dieter Häussinger², Karl S. Lang^{6,+},
8 and Philipp A. Lang^{1,+,*}

9
10 ¹Department of Molecular Medicine II, Medical Faculty, Heinrich Heine University, Universitätsstr. 1, 40225
11 Düsseldorf, Germany, ²Department of Gastroenterology, Hepatology, and Infectious Diseases, Heinrich-Heine-
12 University Düsseldorf, Universitätsstr. 1, 40225 Düsseldorf, Germany, ³Department of Pediatric Oncology,
13 Hematology and Clinical Immunology, Center for Child and Adolescent Health, Heinrich Heine University,
14 Medical Faculty, Duesseldorf, Germany, ⁴Computational Biology of Infection Research, Helmholtz Center for
15 Infection Research, Braunschweig, Germany, ⁵Institute of Virology, TU Munich, Schneckenburgerstr. 8, 81675
16 München, Germany, ⁶Institute of Immunology, Medical Faculty, University of Duisburg-Essen, Hufelandstr. 55,
17 Essen 45147, Germany, ⁷Department of Immunology and Microbial Science, The Scripps Research Institute, La
18 Jolla, CA 92037, USA, ⁸Instituto Andino Patagónico de Tecnologías Biológicas y Geoambientales (IPATEC),
19 Universidad Nacional del Comahue - CONICET, Bariloche, Argentina, ⁹Institute for Virology, University of
20 Duisburg-Essen, Hufelandstr. 55, Essen 45147, Germany, ¹⁰Department of Cell Biology, Vrije University
21 Medical Center, 1081 BT Amsterdam, Netherlands, ¹¹Institute of Medical Microbiology and Hospital Hygiene,
22 Heinrich-Heine-University Duesseldorf, 40225 Duesseldorf, Germany, ¹²Division of Cell Signalling and
23 Immunology, School of Life Sciences, University of Dundee, Dundee DD1 5EH, United Kingdom,
24 ¹³Laboratory of Immune regulation, School of Life Science, Tokyo University of Pharmacy and Life Sciences,
25 1432-1 Horinouchi, Hachioji, Tokyo 192-0392, Japan. ¹⁴Institute of Molecular Immunology, Technische
26 Universität München and Helmholtz Zentrum München, Munich, Germany, ¹⁵Division of Chronic
27 Inflammation and Cancer, German Cancer Research Center (DKFZ), Heidelberg, Germany, ¹⁶Institut für
28 Klinische Chemie und Pathobiochemie, Klinikum rechts der Isar, Technische Universität München, Munich,
29 Germany, ¹⁷Princess Margaret Cancer Center, University Health Network, Toronto, Ontario, Canada M5G 2C1,
30 ¹⁸Department of Infection and Immunity, Experimental and Molecular Immunology, Luxembourg Institute of
31 Health, L-4354 Esch-sur-Alzette, Luxembourg, ¹⁹Odense Research Center for Anaphylaxis (ORCA),
32 Department of Dermatology and Allergy Center, Odense University Hospital, University of Southern Denmark,
33 Odense, Denmark;

34 *Address correspondence to PAL: langp@uni-duesseldorf.de

35 + contributed equally to this work

36 Key words: TNF, MALT1, innate immunity, interferon, NF-κB

37

38 **Abstract**

39 Innate immune activation is essential to mount an effective antiviral response and to
40 prime adaptive immunity. Although a crucial role of CD169⁺ cells during vesicular stomatitis
41 virus (VSV) infections is increasingly recognized, factors regulating CD169⁺ cells during
42 viral infections remain unclear. Here we show that tumor necrosis factor is produced by
43 CD11b⁺ Ly6C⁺Ly6G⁺ cells following infection with VSV. The absence of TNF or TNF
44 receptor 1 (TNFR1) resulted in reduced numbers of CD169⁺ cells and in reduced IFN-I
45 production during VSV infection, with a severe disease outcome. Specifically, TNF triggered
46 RelA translocation into the nucleus of CD169⁺ cells; this translocation was inhibited when
47 paracaspase MALT-1 was absent. Consequently, MALT1 deficiency resulted in reduced
48 VSV replication, defective innate immune activation, and severe disease development. These
49 findings indicate that TNF mediates the maintenance of CD169⁺ cells and innate and
50 adaptive immune activation during VSV infection.

51 **Importance**

52 Over the last decade, strategically placed CD169⁺ metallophilic macrophages in the marginal
53 zone of the murine spleen and LN have been shown to play a very important role in host
54 defense against viral pathogens. CD169⁺ macrophages are shown to activate innate and
55 adaptive immunity via “enforced virus replication” a controlled amplification of virus
56 particles. However, factors regulating the CD169⁺ macrophages remain to be studied. In this
57 paper, we show that after Vesicular stomatitis virus infection, phagocytes produce tumor
58 necrosis factor (TNF) which signals via TNFR1 and promote “enforced virus replication” in

59 CD169⁺ macrophages. Consequently, lack of TNF or TNFR1 resulted in defective immune
60 activation and VSV clearance.

61 Introduction

62 Innate immune activation is crucial for inducing antiviral immunity through cytokine
63 production and adaptive immune priming (1). Splenic marginal zone macrophages and
64 metallophilic marginal zone macrophages play an important role in eliminating blood borne
65 bacterial, parasites and viral pathogens (2, 3). Metallophilic macrophages were originally
66 described when rat splenic marginal zone macrophages were stained with iron and silver
67 impregnation (4). These metallophilic macrophages express the lectin like hemagglutinin
68 CD169, which was identified using a monoclonal antibody: MOMA-1 (5-7). CD169⁺
69 macrophages are increasingly recognized to play a pivotal role in host defense (8). CD169⁺
70 macrophages (referred to as CD169⁺ cells), specifically allow early viral replication to
71 promote innate immune recognition and antigen presentation (9). The absence of CD169⁺
72 cells results in reduced type I interferon (IFN-I) production, reduced B-cell activation, and
73 severe disease development during viral infection (10, 11). B cell-derived lymphotoxin alpha
74 (LT α) and lymphotoxin beta (LT β) drive the maintenance of CD169⁺ cells in spleen and
75 lymph node tissue (10, 12, 13). Consequently, B cell-deficient mice exhibit fewer CD169⁺
76 cells and limited immune activation, including the production of IFN-I (13, 14). However,
77 factors promoting survival and the presence of CD169⁺ cells after viral infection have not yet
78 been sufficiently studied.

79 IFN-I triggers strong inhibitory effects on viral replication and is crucial for
80 preventing severe infections with the vesicular stomatitis virus (VSV) model system (1, 15).
81 This system can be used as a laboratory system for immune recognition during viral
82 infection, as a vaccine vector system, as a tool for viral transduction, and as an oncolytic
83 virus (16, 17). Clearance of VSV depends heavily on IFN-I and the presence of neutralizing

84 antibodies (15, 18). VSV has been used as a murine model of viral infections to study the
85 innate immune response, virus replication in secondary lymphoid organs and the central
86 nervous system (CNS) (19-21). Pathology during VSV infection is seen particularly during
87 infection of the central nervous system (CNS); this pathology includes paralysis and death
88 after infection with VSV (22). Accordingly, mice deficient in IFN- α/β receptor (IFNAR)
89 signaling exhibit paralysis and the presence of VSV in the CNS (15). Consistently, IFN-I can
90 inhibit VSV replication in neurons, and defects in IFN-stimulated genes in the CNS tissue
91 trigger pathology during VSV infection (23, 24). During infection with low doses of VSV,
92 replication of VSV in CD169⁺ cells in the spleen and lymph node tissue is important for
93 inducing protective immunity and preventing CNS infection (9, 10). The VSV backbone is
94 also used during vaccination to induce protective immunity against viruses such as the Ebola
95 virus (25).

96 The role of tumor necrosis factor (TNF) in marginal zone development and marginal
97 zone function is controversial. Although reports show that marginal zone development is
98 impaired and fewer marginal zone macrophages are present in TNF-deficient and p55-TNFR
99 (tumor necrosis factor receptor 1 [TNFR1])-deficient mice (26), other reports suggest that
100 TNF triggers marginal zone macrophage depletion after infection (27, 28). It has also been
101 shown that TNFR1 deficient mice are less susceptible to West Nile virus infection as a result
102 of uncompromised blood brain barrier (29). However, these findings are contradicting other
103 studies utilizing Herpes simplex virus-1 as infection model where it is shown that TNFR1
104 deficient mice are more susceptible to virus infection (30, 31). It is clear that TNF-deficient
105 mice exhibit CD169⁺ cells in the spleen, whereas this cell population is absent in *Lta*^{-/-} mice
106 (26, 27). Furthermore, the production of neutralizing antibodies and the proliferation of

107 antiviral T cells can be induced in TNF-deficient animals (28, 32). These findings suggest
108 that TNF, which is crucial for overcoming bacterial infections (33-36) plays a minor role in
109 antiviral immunity.

110 In this study, we found that absence of TNF reduced the number of CD169⁺ cells,
111 inhibited IFN-I production, and consequently led to a severe disease outcome during
112 infection with VSV. These effects were mainly transmitted by TNFR1 and were dependent
113 on canonical nuclear factor (NF)- κ B.

114 Results

115 TNF production by CD11b⁺Ly6C⁺Ly6G⁺ cells following VSV infection.

116 TNF can be detected during an infection with VSV (32, 37). Consistently, we found
117 that TNF expression levels were higher in the spleen after infection with VSV when
118 compared to uninfected controls (Fig. 1A). Backgating of intracellular TNF producing cells
119 showed that TNF-producing cells are a heterogeneous CD11b⁺ CD19⁻ population (Fig.
120 1B+C). Therefore, we hypothesized that TNF was likely not expressed by B or T cells during
121 infection. Accordingly, we observed TNF mRNA expression levels in *Cd8^{-/-}*, B cell-deficient
122 *Jh^{-/-}*, and *Rag1^{-/-}* mice comparable to WT mice (Fig. 1D). TNF producing cells could be
123 predominantly characterized as CD11b⁺CD11c⁻Ly6C⁺Ly6G⁺MHCII⁺ (Fig. 1E). Consistent
124 with reports that neutrophils (38, 39) and CD11b⁺Ly6C⁺Ly6G⁺ cells (40) are important
125 during early defense against bacterial and viral infections via production of proinflammatory
126 cytokines such as IL1b, IL6, TNF and IFN-I, we found a significant increase of
127 TNF⁺CD11b⁺Ly6C⁺Ly6G⁺ cells (Fig. 1F). Treatment with clodronate liposomes can deplete
128 phagocytic cells in mice (Fig. 1G)(41, 42). Accordingly, clodronate depletion reduced TNF
129 expression after VSV infection suggesting a role of these phagocytic cells in the production
130 of TNF (Fig. 1H). However, when we employed diphtheria toxin- receptor (DTR) induced
131 specific cell depletion of CD169⁺ cells and CD11c⁺ cells; we did not observe reduction in
132 TNF production (Fig.1H). Taken together, these findings indicate that TNF production
133 following intravenous VSV infection is triggered by CD11b⁺CD11c⁻Ly6C⁺Ly6G⁺
134 phagocytes.

135

136 **TNF triggers the maintenance of CD169⁺ cells during viral infection to protect animals**
137 **against the development of severe disease**

138 To determine whether TNF affects the outcome after VSV infection, we infected
139 wild-type (WT) and TNF-deficient mice. TNF-deficient mice developed severe VSV
140 infection in comparison to WT mice (Fig. 2A). Neutralizing antibody titer was achieved later
141 in TNF-deficient mice than in WT mice after infection with low doses of VSV (Fig. 2B).
142 Since IFN-I is critical to overcome an infection with VSV (15), we measured IFN alpha and
143 IFN beta in the serum of infected animals. IFN alpha production was impaired in TNF-
144 deficient mice when compared to control animals (Fig. 2C). However, IFN beta was
145 undetectable in the serum of infected animals when infected with 10⁵ PFU VSV (Fig. 2C).
146 Previous findings show that CD169⁺ cells contribute to innate immune activation not only by
147 allowing viral replication but also by producing IFN-I in mice (10, 43). When we depleted
148 CD169⁺ cells expressing diphtheria toxin receptor (CD169-DTR) by administering diphtheria
149 toxin (DT) (44), we observed reduced IFN-I concentrations in the serum of infected animals
150 (Fig. 2D). To exclude the possibility of defective innate Toll-like receptor (TLR) activation,
151 we administered the TLR3 agonist poly I:C. We found that the IFN-I production was intact in
152 both WT and TNF-deficient mice (Fig. 2E). Hence, we speculated that TNF promoted the
153 function of CD169⁺ cells and thus contributed to IFN-I production following VSV infection.
154 Shortly after infection with VSV, the number of CD169⁺ cells in spleen tissue decreased in
155 TNF-deficient mice when compared to spleen tissue harvested from WT animals (Fig. 2F-H).
156 To understand the reduced production of IFN-I in absence of TNF, we monitored the virus
157 replication in spleen tissue of WT and *Tnfa*^{-/-} mice. The expression of VSV glycoprotein
158 (VSV-G) was detected in lower quantities in spleen tissue harvested from TNF-deficient

159 animals compared to WT mice after VSV infection (Fig. 2I+J). Consistently, early VSV titers
160 after infection were lower in *Tnfa*^{-/-} mice than in control mice, a condition that negatively
161 affects antiviral immune activation (Fig. 2K). Injection of ultraviolet light (UV)-inactivated
162 virus could increase TNF mRNA expression in WT mice (Fig. 2L). However, decrease of
163 CD169⁺ cells was dependent on live virus, because UV-inactivated virus did not affect
164 CD169⁺ cells in spleen tissue of *Tnfa*^{-/-} mice (Fig. 2M). These findings indicate that TNF is
165 necessary to sustain virus replication in early hours of infection but is dispensable for sterile
166 innate immune activation. Notably, *CD169*^{-/-} mice exhibited VSV-G expression in spleen
167 tissue, a finding indicating that downregulation of the protein CD169 would not cause
168 absence of virus replication (Fig. 2N). Taken together, these findings indicate that the
169 absence of TNF results in defective antiviral innate immune activation after infection with
170 VSV.

171

172 **CD169⁺ cell maintenance via TNFR1 results in productive VSV replication and** 173 **immune activation**

174 To further characterize the role of TNF during viral infection, we infected TNFR1-
175 and TNFR2-deficient mice with VSV. In line with findings from TNF-deficient animals, the
176 absence of TNFR1 but not that of TNFR2 resulted in a decrease in the number of CD169⁺
177 cells in spleen tissue (Fig. 3A + B). Furthermore, VSV-G production was lower in *Tnfrsf1a*^{-/-}
178 animals than in WT or *Tnfrsf1b*^{-/-} mice (Fig. 3A). Consistently, VSV titers were reduced in
179 spleen tissue shortly after infection in *Tnfrsf1a*^{-/-} animals, in sharp contrast to the findings in
180 WT and *Tnfrsf1b*^{-/-} mice (Fig. 3C). Interestingly, IFN-I production was defective in *Tnfrsf1a*^{-/-}

181 ^{-/-} mice but was also lower in *Tnfrsf1b*^{-/-} animals than in WT control mice (Fig. 3D). IFN-I is
182 necessary for the expression of anti-virally active IFN-stimulated genes (ISGs) (1).
183 Consistently, we found reduced expression of ISGs in the CNS of *Tnfrsf1a*^{-/-} mice after
184 infection with VSV (Fig. 3E). Defective ISG expression was not found to the same extent in
185 *Tnfrsf1b*^{-/-} CNS tissue (Fig. 3F). VSV can drive neuropathological symptoms by infecting
186 the CNS (22). When we measured viral titers in the spinal cord and brain tissue of mice
187 exhibiting hind leg paralysis, we found infectious VSV in tissue from TNFR1-deficient mice
188 (Figure 3G). Consequently, *Tnfrsf1a*^{-/-} mice developed clinical signs of CNS infection,
189 unlike WT and *Tnfrsf1b*^{-/-} mice (Fig. 3H). Taken together, these findings suggest that TNFR1
190 drives antiviral defense by promoting CD169⁺ cell survival.

191

192 **TNFR1 triggers the survival of CD169⁺ cells**

193 Next, we opted to determine which factors drive the maintenance of CD169⁺ cells and
194 enforced viral replication after viral infection. B cell-mediated Ltβ production is important
195 for splenic CD169⁺ cells. Hence, we wondered whether the defects in absence of TNF were
196 triggered by B cells. Notably, we did not observe any major changes of B-cell subsets in
197 TNF, TNFR1 or TNFR2-deficient mice (Fig. 4A). Consistently, we did not see differential
198 expression of *Lta*, *Ltβ*, or Ltβ receptor (*LtbR*) in TNFR1-deficient mice (Fig. 4B).
199 Additionally, we found no major differences in B-cell subsets between WT and *Tnfrsf1a*^{-/-}
200 mice after infection (Fig. 4C). Furthermore, we reconstituted lethally irradiated C57BL/6
201 mice with mixed bone marrow from *Rag1*^{-/-} and *Tnfrsf1a*^{-/-} and *Rag1*^{-/-} and WT donors at a
202 ratio of 1:1. Mice reconstituted with *Rag1*^{-/-}: *Tnfrsf1a*^{-/-} bone marrow exhibited no

203 significant reduction in IFN- α in the serum when compared to mice reconstituted with *Rag1*^{-/-}
204 ^{-/-}; WT bone marrow (Fig. 4D). Furthermore, there was no difference between these mice in
205 neutralizing antibody production (Fig. 4E). To elucidate if TNFR1 deficiency specifically on
206 CD169⁺ cells have a role in virus replication, we reconstituted lethally irradiated C57BL/6
207 mice with mixed bone marrow from CD169-DTR⁺ and *Tnfrsf1a*^{-/-} donors as well as CD169-
208 DTR⁺ and WT donors at a ratio of 1:1. We observed that the production of IFN- α was lower
209 in the mice reconstituted with CD169-DTR⁺ + *Tnfrsf1a*^{-/-} bone marrow compared to control
210 mice reconstituted with CD169-DTR⁺ + WT after infection with VSV and DT treatment (Fig.
211 4F). Furthermore, we found slightly delayed presence of VSV neutralizing antibody titers in
212 CD169-DTR⁺:*Tnfrsf1a*^{-/-} recipients when compared to corresponding CD169-DTR⁺:WT
213 recipients (Fig. 4G). CD169⁺ cells can be depleted in CD11c-DTR mice, because CD169⁺
214 cells exhibit intermediate expression of CD11c (10, 45). Consistently, lethally irradiated mice
215 reconstituted with mixed bone marrow from CD11c-DTR⁺ and *Tnfrsf1a*^{-/-} mice exhibited
216 reduced concentrations of IFN- α after VSV infection when compared to CD11c-DTR⁺:WT
217 recipients (Fig. 4H). These findings suggest that TNFR1 triggers cell-intrinsic effects on
218 CD169⁺ cells.

219 We speculated that TNF delivers an important survival signal for CD169⁺ cells. To
220 determine if TNF is involved in protection against VSV induced apoptosis, we measured
221 caspase 3 activity on whole spleen tissue lysates. After VSV infection caspase 3 activity was
222 significantly higher in *Tnfa*^{-/-} mice compared to control animals (Fig. 5A). VSV is known to
223 induce apoptosis and inactivates Mcl-1 and Bcl-Xl (46). To elucidate if TNF plays a role in
224 promoting expression of anti-apoptotic genes, we measured mRNA expression of *Bcl2*, *Bcl-*
225 *XL* and *xIAP* in spleen tissue of mice after VSV infection (Fig. 5B). After VSV infection,

226 *Bcl2* and *Bcl-Xl* expression was significantly reduced in *Tnfa*^{-/-} mice compared to WT mice
227 (Fig. 5B). To enumerate the mechanism which reduces CD169⁺ cells in TNF deficient mice
228 after infection we made use of terminal deoxynucleotidyl transferase dUTP nick end
229 labelling (TUNEL) assay. The number as well as the mean fluorescence intensity of TUNEL-
230 positive CD169⁺ cells was higher in spleen tissue from TNF deficient mice than in tissue
231 from corresponding WT control mice (Fig. 5C+D). The proportion of CD169⁺ cells that
232 stained positive for 7-aminoactinomycin D (7-AAD) was higher in TNFR1-deficient mice
233 than in WT control mice 8h after infection (Fig. 5E). Next, we wondered if we can rescue the
234 CD169⁺ cells by injecting the pan-caspase inhibitor Z-Val-Ala-Asp-fluoromethylketone
235 (zVAD-FMK). Z-VAD treatment restored the presence of CD169⁺ cells in TNF-deficient
236 animals, a finding indicating that CD169⁺ cells depend on TNF-mediated survival (Fig.
237 5F+G). Although treatment of TNF-deficient mice with Z-VAD rescued CD169⁺ cells, it
238 failed to rescue the IFN-I response suggesting the role of TNF signaling is not only essential
239 to prevent apoptosis, but also for IFN-I production (Fig. 5H). In summary, these findings
240 indicate that TNF delivers a survival signal that is important for the maintenance of CD169⁺
241 cells in the spleen after viral infection and IFN-I production.

242

243 **The NF-κB regulator MALT1 promotes canonical NF-κB expression, VSV replication**
244 **in CD169⁺ cells, and immune activation during viral infection**

245 TNF can induce NF-κB activation via TNFR1 and can promote the expression of
246 genes driving survival and of proinflammatory cytokines (47). Furthermore, TNF is known to
247 promote IFN-I production (48). Consistently, RelA expression was increased in the marginal

248 zone of spleen tissue after VSV infection (Fig. 6A). We quantified cytoplasmic and nuclear
249 expression of RelA in CD169⁺ cells. Nuclear presence of RelA in CD169⁺ cells was higher in
250 VSV-infected mice than in naïve controls (Fig. 6B). We wondered whether nuclear *RelA*
251 expression was dependent on TNF. As expected, compared with WT control mice, VSV-
252 infected mice exhibited reduced expression of RelA in the nuclear compartment of CD169⁺
253 cells in absence of TNF (Fig. 6C). Notably, the presence of RelA was reduced in TNFR1
254 deficient mice, but we observed no difference in RelA expression between TNFR2-deficient
255 mice and corresponding control mice (Fig. 6D+E). It has been reported that one of the major
256 regulator of RelA signaling is RelB which acts through sequestration of RelA in the
257 cytoplasm and competitive binding of DNA (49). It is also reported that the paracaspase
258 MALT1 can promote canonical NF-κB signaling by cleaving RelB (50, 51). Hence, we
259 stained spleen sections of *Malt1*^{+/-} and *Malt1*^{-/-} mice for RelB. Ablation of MALT1 resulted
260 in increased levels of RelB in CD169⁺ cells in the marginal zone of the spleen (Fig. 7A+B).
261 In turn, nuclear RelA levels were lower in CD169⁺ cells in *Malt1*^{-/-} spleen tissue than in
262 control tissue (Fig. 7C). Consistently, mouse embryonic fibroblasts (MEFs) derived from
263 *Malt1*^{-/-} mice showed reduced translocation of p65 into the nucleus after stimulation with
264 TNF but higher expression of RelB in the nucleus (Fig. 7D+E). These findings indicate that
265 MALT1 destabilizes RelB in marginal zone macrophages to promote canonical NF-κB
266 signaling. The presence of CD169⁺ cells in spleen tissue was not affected by *Malt1* before or
267 after infection with VSV (Fig. 8A). However, the expression of VSV-G was lower in *Malt1*^{-/-}
268 mice than in control mice (Fig. 8B+C). Consistently, the number of infectious VSV particles
269 were lower in spleen tissue harvested from *Malt1*^{-/-} mice than in spleen tissue from control
270 mice (Fig. 8D). Hence, IFN-I serum concentrations after VSV infection were lower in

271 MALT1 deficient mice than in control mice (Fig. 8E). A previous report suggests that
272 MALT1 is not required for RIG-I activation (52). Consistently, when we injected polyI:C
273 into *Malt1*^{+/-} and *Malt1*^{-/-} mice, we found similar serum IFN-I levels in both groups (Fig.
274 8F). Hence we concluded that defective IFN-I production during VSV infection was caused
275 by reduced VSV replication early during infection. Consequently, MALT1 deficient mice
276 succumbed to the infection in sharp contrast to control animals (Fig. 8G).

277 Taken together, these findings indicate that absence of MALT1 results in reduced
278 canonical NF-κB signaling in response to VSV infection. *Malt1*-deficient mice exhibit
279 reduced VSV replication and immune activation.

280 **Discussion**

281 In this study, we found that TNF plays a crucial role in the maintenance of CD169⁺
282 cells early after infection with VSV. Consequently, TNF, TNFR1, and MALT1 deficient
283 animals exhibited reduced immune activation, limited IFN-I production, which consequently
284 led to a severe VSV infection.

285 The role of TNF during viral infection is controversial and not sufficiently
286 understood. Although reports describe activating polymorphisms in TNF, which are
287 associated with the establishment of a chronic viral infection (53), other reports state that the
288 same mutations are protective against chronic hepatitis B virus infection (HBV) (54). *In*
289 *vitro*, TNF can propagate the viral replication of HCV (55) although HCV increases the
290 incidence of TNF-induced apoptosis (56). On the other hand, TNF strongly inhibits influenza
291 virus replication in porcine lung epithelial cells (57). Consistently, the attenuation of TNF
292 signaling in a murine T cell-independent model of HBV infection results in viral persistence
293 (58). In turn, the application of Smac mimetics enhances TNF signaling and is associated
294 with increased clearance of HBV in this model system (59). During infection with VSV, the
295 production of neutralizing antibodies is not defective in the absence of TNFR1 (32).
296 Moreover, TNF can induce T-cell dysfunction and, therefore, promote chronic viral infection
297 (60). Our findings that TNF is crucial for the maintenance of CD169⁺ cells in spleen tissue
298 may be important for infections with lower doses of virus, because allowing viral replication
299 in CD169⁺ cells is particularly important for protective adaptive immunity (9, 13). This may
300 be crucial for the maintenance of CD169⁺ cells in spleen tissue during vaccination with
301 attenuated virus strains or VSV vector-based vaccines (25). These findings may not only be

302 specific for splenic CD169⁺ cells, since intranasal infection with recombinant TNF
303 overexpressing Rabies virus (RV), reduced RV load and mortality (61).

304 Viral replication in CD169⁺ cells, which is promoted by TNF, contributes to
305 improved antigen presentation. CD169⁺ cells in the marginal zone are in close contact with
306 pathogens and are ideally situated to induce an immune response (62). Furthermore, CD169⁺
307 cells have been shown not only to present antigens to B cells in the lymph nodes but also to
308 prime T cells (11, 63). Moreover, CD169⁺ cells are important for virus-mediated IFN-I
309 production which prevents severe CNS infection in mice (64). Our findings show that TNF
310 promotes maintenance of CD169⁺ cells and IFN-I production following VSV infection.
311 Furthermore, our findings show that the translocation of RelA to the nuclei of CD169⁺ cells
312 after VSV infection is dependent on TNF. It has been postulated that canonical NF-κB can
313 contribute to the production of IFN-α (65, 66). However, RelA-deficient and p50-deficient
314 MEFs can produce IFN-α after viral infection, whereas only early IFN-I transcription is
315 reduced (67, 68). Furthermore, RelA-deficient plasmacytoid dendritic cells (pDCs) exhibited
316 reduced IFN production after exposure to Sendai virus (69). Our findings indicate that
317 canonical NF-κB activation can also promote early viral replication and consequently
318 contribute to the production of IFN-I. Consistently, non-canonical NF-κB, which can inhibit
319 canonical NF-κB signaling, is a potent inhibitor of IFN-I production (70). Hence, the
320 paracaspase MALT1, which can cleave RelB and consequently promote canonical NF-κB
321 signaling (50, 51) is necessary for the sufficient propagation of VSV replication and IFN-I
322 production.

323 Taken together, we have found that TNF-TNFR1 signaling is crucial for protecting
324 CD169⁺ cells and their function in innate immune activation during VSV infection.

325 **Materials and Methods:**

326 **Mice, viruses, virus titration:** *Tnfa*^{-/-}, *Tnfrsf1b*^{-/-}, *Cd8*^{-/-} and *Rag1*^{-/-} mice were purchased
327 from Jackson Laboratories (United States). *Tnfrsf1a*^{-/-} mice have been previously described
328 (34). *Malt1*^{-/-}, *CD169*^{-/-}, CD169-DTR, and CD11c-DTR mice have also been previously
329 described (71-74). All mice were maintained on a C57BL/6 genetic background. VSV
330 Indiana strain (VSV-IND, strain Mudd-Summers) was originally obtained from Prof. D.
331 Kolakofsky (University of Geneva, Switzerland). VSV was propagated and titrated as
332 previously described (13). Mice were infected with VSV via tail vein injection. In survival
333 experiments, mice exhibiting symptoms of hind leg paralysis were considered severe, taken
334 out of the experiment, and counted as dead. Blood was collected at the indicated time points
335 after infection. VSV neutralizing antibody titers were measured by plaque reduction
336 neutralization test (PRNT) as previously described (9, 13). Briefly, serum samples were
337 diluted 1:40 and incubated at 56°C for 30 min. To evaluate IgG, serum was pretreated with
338 0.1M β-mercaptoethanol. Serial 2 fold dilutions were performed for 12 steps and incubated
339 with 5000 PFU of VSV. Virus and serum mixture was incubated on a Vero cell monolayer.
340 Plates were stained with crystal violet after 24h. To inhibit caspase activity *in vivo*, we
341 administered three doses (2 μg/g each) of zVAD-FMK (Abcam, Cambridge, UK) (75, 76).
342 For chimera experiments, mice were lethally irradiated with 10.2 Gy. After 24 h, mixed bone
343 marrow from WT or *Tnfrsf1a*^{-/-} and CD169-DTR, CD11c-DTR, and *Rag1*^{-/-} mice was
344 transplanted into the irradiated mice as indicated. All mice were maintained under specific
345 pathogen-free conditions at the authorization of the Landesamt für Natur, Umwelt und
346 Verbraucherschutz of North Rhine-Westphalia (LANUV NRW) in accordance with the
347 German laws for animal protection.

348 **Depletion of cells:** To deplete macrophages, 200ul clodronate liposomes was injected
349 intravenously, 24h later mice were infected with VSV. Clodronate was provided by Nico van
350 Rooijen and used as previously described (41, 42)(Vrije University Medical Center,
351 Netherlands). CD169⁺ and CD11c⁺ expressing cells in CD169-DTR and CD11c-DTR mice
352 were depleted by injecting 2 doses of 100ng diphtheria toxin (DT) (Sigma) 1 day before and
353 at the day of infection.

354

355 **Histology and ELISA:** Histological analysis of snap-frozen tissue was performed as
356 previously described (9). Briefly, Snap-frozen tissue sections were cut in 7µm thickness, air
357 dried and fixed with acetone for 10min. Sections were blocked with 2% fetal calf serum in
358 PBS for 1h. Sections were stained with anti-CD169 (final conc. 4 µg/ml) (Acris, Germany;
359 clone: MOMA-1), anti-VSV-G (final conc. 1 µg/ml) (produced in-house, clone: Vi10), anti-
360 RelA (final conc. 1µg/ml) (Santa Cruz Biotechnology, USA), anti-F4/80 (final conc. 2µg/ml)
361 (eBioscience, clone BM8) and anti-RelB (final conc. 1µg/ml) (Cell Signaling, USA;
362 polyclonal) for 1h. Then Sections were washed with PBS containing 0.05% Tween 20
363 (Sigma). Secondary antibodies, PE streptavidin (final conc. 1µg/ml) (eBioscience), anti-
364 Rabbit FITC (final conc. 1µg/ml) (Thermofisher), anti-Goat FITC (final conc. 1µg/ml) (Santa
365 Cruz Biotechnology, USA) were incubated for 1h. Then sections were washed with PBS
366 containing 0.05% Tween 20 (Sigma) and mounted using fluorescence mounting medium
367 (Dako). Caspase 3 activity assay was performed with a fluorescence assay according to the
368 manufacturer's instructions (Cell Signaling). TUNEL staining was performed on formalin-
369 fixed spleen sections according to the manufacturer's instructions (Thermo scientific, USA).
370 Images were obtained with a LSM510 confocal microscope and Axio Observer Z1

371 fluorescence microscope (Zeiss, Germany). Analysis of the fluorescence images was
372 performed with ImageJ software. IFN- α and IFN- β (PBL Biosciences, New Jersey, USA)
373 concentrations were determined using enzyme-linked immunosorbent assay (ELISA)
374 according to the manufacturers' instructions.

375 **RT-PCR analyses:** RNA purification was performed according to manufacturer's
376 instructions (Qiagen RNeasy Kit or Trizol). Gene expression of *Bcl2*, *Bcl-xl*, *Xiap*, *Lta*, *Ltb*,
377 *Ifit1*, *Ifit2*, *Ifit3*, *Irf7*, *Isg15*, *Oasl1* and *Tnfa*, was performed using FAM/VIC probes (Applied
378 Biosystems) and iTAQ™ One step PCR kit (Bio rad). For analysis, the expression levels of
379 all target genes were normalized to β -actin/GAPDH expression (Δ Ct). Gene expression
380 values were then calculated based on the $\Delta\Delta$ Ct method, using naive WT mice as a control to
381 which all other samples were compared. Relative quantities (RQ) were determined using the
382 equation: $RQ=2^{-\Delta\Delta Ct}$.

383 **Immunoblotting:** *Malt1*^{+/-} and *Malt1*^{-/-} mouse embryonic fibroblasts (MEFs) were obtained
384 from Jürgen Ruland (Technische Universität München, Germany). *Malt1*^{+/-} and *Malt1*^{-/-}
385 MEFs were stimulated with 100 ng/ml murine-soluble TNF (mTNF; R&D Systems).
386 Cytoplasmic and nuclear extracts were prepared according to manufacturer's instructions
387 (Active Motif, Belgium). Immunoblots were probed with primary anti-p65 (Santa Cruz
388 Biotechnology), anti-RelB (Cell Signaling), and anti-p100/p52 (Cell Signaling).

389 **Flow cytometry:** For intracellular cytokine staining, single-cell suspended splenocytes were
390 incubated with Brefeldin A (eBioscience), followed by an additional 5 h of incubation at
391 37°C. After surface staining with anti-CD3, anti-CD8, anti-CD11b, anti-CD11c, anti-CD19,

392 anti-CD115, anti-F4/80, anti-Ly6C, anti-Ly6G anti-MHC-II, and anti-NK1.1 antibodies (all
393 from eBioscience), cells were fixed with 2% formalin, permeabilized with 0.1% saponin, and
394 stained with anti-TNF antibodies (eBioscience) for 30 min at 4°C. B-cell subsets were
395 detected in single-cell suspensions of splenocytes with anti-CD5, anti-CD19, anti-CD21,
396 anti-CD23, and anti-immunoglobulin M (IgM) antibodies (all from eBioscience). BD
397 Calibrite™ (BD Biosciences, USA) beads were added to the samples before acquisition by BD
398 LSRFortessa™.

399

400 **Statistical analyses:** Data are represented as +SEM or ±SEM. Statistically significant
401 differences between two groups were determined with Student's *t*-test. Statistically
402 significant differences between several groups were determined by one-way analysis of
403 variance (ANOVA) with additional Bonferroni or Dunnett post hoc test. Statistically
404 significant differences between groups in experiments involving more than one time-point
405 were determined with two-way ANOVA (repeated measurements).

406

407 **Acknowledgements:**

408 We thank Flo Witte for valuable comments on the manuscript. This study was supported by
409 the Alexander von Humboldt Foundation (SKA2010), the German Research Council
410 (SFB974, LA2558/3-1, LA2558/5-1, GRK1949 & TRR60), the Jürgen Manchot Graduate
411 School MOI II, and the NIH tetramer facility. D.B.is funded by the ATTRACT Programme
412 (A14/BM/7632103/DBRRIL) and a CORE grant (C15/BM/10355103) of the National
413 Research Fund Luxembourg (FNR).

414

415

416

417

418 **References:**

- 419 1. McNab F, Mayer-Barber K, Sher A, Wack A, O'Garra A. 2015. Type I interferons in
420 infectious disease. *Nat Rev Immunol* 15:87-103.
- 421 2. Chavez-Galan L, Ollerios ML, Vesin D, Garcia I. 2015. Much More than M1 and M2
422 Macrophages, There are also CD169(+) and TCR(+) Macrophages. *Front Immunol*
423 6:263.
- 424 3. Mebius RE, Kraal G. 2005. Structure and function of the spleen. *Nat Rev Immunol*
425 5:606-16.
- 426 4. Snook T. 1964. Studies on the Perifollicular Region of the Rat's Spleen. *Anat Rec*
427 148:149-59.
- 428 5. Crocker PR, Gordon S. 1986. Properties and distribution of a lectin-like
429 hemagglutinin differentially expressed by murine stromal tissue macrophages. *J Exp*
430 *Med* 164:1862-75.
- 431 6. Kraal G, Janse M. 1986. Marginal metallophilic cells of the mouse spleen identified
432 by a monoclonal antibody. *Immunology* 58:665-9.
- 433 7. Oetke C, Kraal G, Crocker PR. 2006. The antigen recognized by MOMA-I is
434 sialoadhesin. *Immunol Lett* 106:96-8.
- 435 8. Gupta P, Lai SM, Sheng J, Tetlak P, Balachander A, Claser C, Renia L, Karjalainen
436 K, Ruedl C. 2016. Tissue-Resident CD169(+) Macrophages Form a Crucial Front
437 Line against Plasmodium Infection. *Cell Rep* 16:1749-61.
- 438 9. Honke N, Shaabani N, Cadeddu G, Sorg UR, Zhang DE, Trilling M, Klingel K,
439 Sauter M, Kandolf R, Gailus N, van Rooijen N, Burkart C, Baldus SE, Grusdat M,
440 Lohning M, Hengel H, Pfeffer K, Tanaka M, Haussinger D, Recher M, Lang PA,
441 Lang KS. 2012. Enforced viral replication activates adaptive immunity and is
442 essential for the control of a cytopathic virus. *Nature Immunology* 13:51-7.
- 443 10. Iannacone M, Moseman EA, Tonti E, Bosurgi L, Junt T, Henrickson SE, Whelan SP,
444 Guidotti LG, von Andrian UH. 2010. Subcapsular sinus macrophages prevent CNS
445 invasion on peripheral infection with a neurotropic virus. *Nature* 465:1079-83.
- 446 11. Junt T, Moseman EA, Iannacone M, Massberg S, Lang PA, Boes M, Fink K,
447 Henrickson SE, Shayakhmetov DM, Di Paolo NC, van Rooijen N, Mempel TR,
448 Whelan SP, von Andrian UH. 2007. Subcapsular sinus macrophages in lymph nodes
449 clear lymph-borne viruses and present them to antiviral B cells. *Nature* 450:110-4.
- 450 12. Tumanov A, Kuprash D, Lagarkova M, Grivennikov S, Abe K, Shakhov A,
451 Drutskaya L, Stewart C, Chervonsky A, Nedospasov S. 2002. Distinct role of surface
452 lymphotoxin expressed by B cells in the organization of secondary lymphoid tissues.
453 *Immunity* 17:239-50.
- 454 13. Xu HC, Huang J, Khairnar V, Duhan V, Pandya AA, Grusdat M, Shinde P,
455 McIlwain DR, Maney SK, Gommerman J, Lohning M, Ohashi PS, Mak TW, Pieper
456 K, Sic H, Speletas M, Eibel H, Ware CF, Tumanov AV, Kruglov AA, Nedospasov

- SA, Haussinger D, Recher M, Lang KS, Lang PA. 2015. Deficiency of the B cell-activating factor receptor results in limited CD169+ macrophage function during viral infection. *J Virol* 89:4748-59.
14. Khairnar V, Duhan V, Maney SK, Honke N, Shaabani N, Pandya AA, Seifert M, Pozdeev V, Xu HC, Sharma P, Baldin F, Marquardsen F, Merches K, Lang E, Kirschning C, Westendorf AM, Haussinger D, Lang F, Dittmer U, Kuppers R, Recher M, Hardt C, Scheffrahn I, Beauchemin N, Gothert JR, Singer BB, Lang PA, Lang KS. 2015. CEACAM1 induces B-cell survival and is essential for protective antiviral antibody production. *Nat Commun* 6:6217.
15. Muller U, Steinhoff U, Reis LF, Hemmi S, Pavlovic J, Zinkernagel RM, Aguet M. 1994. Functional role of type I and type II interferons in antiviral defense. *Science* 264:1918-21.
16. Kawai T, Akira S. 2009. The roles of TLRs, RLRs and NLRs in pathogen recognition. *Int Immunol* 21:317-37.
17. Lichty BD, Power AT, Stojdl DF, Bell JC. 2004. Vesicular stomatitis virus: re-inventing the bullet. *Trends Mol Med* 10:210-6.
18. Hangartner L, Zinkernagel RM, Hangartner H. 2006. Antiviral antibody responses: the two extremes of a wide spectrum. *Nat Rev Immunol* 6:231-43.
19. Bi Z, Barna M, Komatsu T, Reiss CS. 1995. Vesicular stomatitis virus infection of the central nervous system activates both innate and acquired immunity. *J Virol* 69:6466-72.
20. Chauhan VS, Furr SR, Sterka DG, Jr., Nelson DA, Moerdyk-Schauwecker M, Marriott I, Grdzlishvili VZ. 2010. Vesicular stomatitis virus infects resident cells of the central nervous system and induces replication-dependent inflammatory responses. *Virology* 400:187-96.
21. Christian AY, Barna M, Bi Z, Reiss CS. 1996. Host immune response to vesicular stomatitis virus infection of the central nervous system in C57BL/6 mice. *Viral Immunol* 9:195-205.
22. Huneycutt BS, Bi Z, Aoki CJ, Reiss CS. 1993. Central neuropathogenesis of vesicular stomatitis virus infection of immunodeficient mice. *J Virol* 67:6698-706.
23. Fensterl V, Wetzel JL, Ramachandran S, Ogino T, Stohlman SA, Bergmann CC, Diamond MS, Virgin HW, Sen GC. 2012. Interferon-induced Ifit2/ISG54 protects mice from lethal VSV neuropathogenesis. *PLoS Pathog* 8:e1002712.
24. Trotter MD, Jr., Palian BM, Reiss CS. 2005. VSV replication in neurons is inhibited by type I IFN at multiple stages of infection. *Virology* 333:215-25.
25. Jones SM, Feldmann H, Stroher U, Geisbert JB, Fernando L, Grolla A, Klenk HD, Sullivan NJ, Volchkov VE, Fritz EA, Daddario KM, Hensley LE, Jahrling PB, Geisbert TW. 2005. Live attenuated recombinant vaccine protects nonhuman primates against Ebola and Marburg viruses. *Nat Med* 11:786-90.
26. Pasparakis M, Kousteni S, Peschon J, Kollias G. 2000. Tumor necrosis factor and the p55TNF receptor are required for optimal development of the marginal sinus and for migration of follicular dendritic cell precursors into splenic follicles. *Cell Immunol* 201:33-41.
27. Engwerda CR, Ato M, Cotterell SE, Mynott TL, Tschannerl A, Gorak-Stolinska PM, Kaye PM. 2002. A role for tumor necrosis factor-alpha in remodeling the splenic marginal zone during *Leishmania donovani* infection. *Am J Pathol* 161:429-37.

- 503 28. Calzascia T, Pellegrini M, Hall H, Sabbagh L, Ono N, Elford AR, Mak TW, Ohashi
504 PS. 2007. TNF-alpha is critical for antitumor but not antiviral T cell immunity in
505 mice. *J Clin Invest* 117:3833-45.
- 506 29. Wang T, Town T, Alexopoulou L, Anderson JF, Fikrig E, Flavell RA. 2004. Toll-like
507 receptor 3 mediates West Nile virus entry into the brain causing lethal encephalitis.
508 *Nat Med* 10:1366-73.
- 509 30. Lundberg P, Welander PV, Edwards CK, 3rd, van Rooijen N, Cantin E. 2007. Tumor
510 necrosis factor (TNF) protects resistant C57BL/6 mice against herpes simplex virus-
511 induced encephalitis independently of signaling via TNF receptor 1 or 2. *J Virol*
512 81:1451-60.
- 513 31. Vilela MC, Lima GK, Rodrigues DH, Lacerda-Queiroz N, Mansur DS, de Miranda
514 AS, Rachid MA, Kroon EG, Vieira LQ, Campos MA, Teixeira MM, Teixeira AL.
515 2010. TNFR1 plays a critical role in the control of severe HSV-1 encephalitis.
516 *Neurosci Lett* 479:58-62.
- 517 32. Fehr T, Bachmann MF, Bluethmann H, Kikutani H, Hengartner H, Zinkernagel RM.
518 1996. T-independent activation of B cells by vesicular stomatitis virus: no evidence
519 for the need of a second signal. *Cell Immunol* 168:184-92.
- 520 33. Rothe J, Lesslauer W, Lotscher H, Lang Y, Koebel P, Kontgen F, Althage A,
521 Zinkernagel R, Steinmetz M, Bluethmann H. 1993. Mice lacking the tumour necrosis
522 factor receptor 1 are resistant to TNF-mediated toxicity but highly susceptible to
523 infection by *Listeria monocytogenes*. *Nature* 364:798-802.
- 524 34. Pfeffer K, Matsuyama T, Kundig TM, Wakeham A, Kishihara K, Shahinian A,
525 Wiegmann K, Ohashi PS, Kronke M, Mak TW. 1993. Mice deficient for the 55 kd
526 tumor necrosis factor receptor are resistant to endotoxic shock, yet succumb to *L.*
527 *monocytogenes* infection. *Cell* 73:457-67.
- 528 35. Botha T, Ryffel B. 2003. Reactivation of latent tuberculosis infection in TNF-
529 deficient mice. *J Immunol* 171:3110-8.
- 530 36. Wellmer A, Gerber J, Ragheb J, Zysk G, Kunst T, Smirnov A, Bruck W, Nau R.
531 2001. Effect of deficiency of tumor necrosis factor alpha or both of its receptors on
532 *Streptococcus pneumoniae* central nervous system infection and peritonitis. *Infect*
533 *Immun* 69:6881-6.
- 534 37. Bartholdy C, Nansen A, Marker O, Thomsen AR. 1999. Soluble tumour necrosis
535 factor (TNF)-receptor levels in serum as markers of anti-viral host reactivity. *Clin*
536 *Exp Immunol* 116:299-306.
- 537 38. Brandes M, Klauschen F, Kuchen S, Germain RN. 2013. A systems analysis
538 identifies a feedforward inflammatory circuit leading to lethal influenza infection.
539 *Cell* 154:197-212.
- 540 39. Petrofsky M, Bermudez LE. 1999. Neutrophils from *Mycobacterium avium*-infected
541 mice produce TNF-alpha, IL-12, and IL-1 beta and have a putative role in early host
542 response. *Clin Immunol* 91:354-8.
- 543 40. Fischer MA, Davies ML, Reider IE, Heipertz EL, Epler MR, Sei JJ, Ingersoll MA,
544 Rooijen NV, Randolph GJ, Norbury CC. 2011. CD11b(+), Ly6G(+) cells produce
545 type I interferon and exhibit tissue protective properties following peripheral virus
546 infection. *PLoS Pathog* 7:e1002374.
- 547 41. Stienstra R, Saudale F, Duval C, Keshtkar S, Groener JE, van Rooijen N, Staels B,
548 Kersten S, Muller M. 2010. Kupffer cells promote hepatic steatosis via interleukin-

- 549 1beta-dependent suppression of peroxisome proliferator-activated receptor alpha
550 activity. *Hepatology* 51:511-22.
- 551 42. Van Rooijen N, Sanders A. 1996. Kupffer cell depletion by liposome-delivered drugs:
552 comparative activity of intracellular clodronate, propamide, and
553 ethylenediaminetetraacetic acid. *Hepatology* 23:1239-43.
- 554 43. Garcia Z, Lemaitre F, van Rooijen N, Albert ML, Levy Y, Schwartz O, Bousso P.
555 2012. Subcapsular sinus macrophages promote NK cell accumulation and activation
556 in response to lymph-borne viral particles. *Blood* 120:4744-50.
- 557 44. Asano K, Nabeyama A, Miyake Y, Qiu CH, Kurita A, Tomura M, Kanagawa O, Fujii
558 S, Tanaka M. 2011. CD169-positive macrophages dominate antitumor immunity by
559 crosspresenting dead cell-associated antigens. *Immunity* 34:85-95.
- 560 45. Probst HC, Tschannen K, Odermatt B, Schwendener R, Zinkernagel RM, Van Den
561 Broek M. 2005. Histological analysis of CD11c-DTR/GFP mice after in vivo
562 depletion of dendritic cells. *Clin Exp Immunol* 141:398-404.
- 563 46. Pearce AF, Lyles DS. 2009. Vesicular stomatitis virus induces apoptosis primarily
564 through Bak rather than Bax by inactivating Mcl-1 and Bcl-XL. *J Virol* 83:9102-12.
- 565 47. Brenner D, Blaser H, Mak TW. 2015. Regulation of tumour necrosis factor
566 signalling: live or let die. *Nat Rev Immunol* 15:362-74.
- 567 48. Basagoudanavar SH, Thapa RJ, Nogusa S, Wang J, Beg AA, Balachandran S. 2011.
568 Distinct roles for the NF-kappa B RelA subunit during antiviral innate immune
569 responses. *J Virol* 85:2599-610.
- 570 49. Marienfeld R, May MJ, Berberich I, Serfling E, Ghosh S, Neumann M. 2003. RelB
571 forms transcriptionally inactive complexes with RelA/p65. *J Biol Chem* 278:19852-
572 60.
- 573 50. Hailfinger S, Nogai H, Pelzer C, Jaworski M, Cabalzar K, Charton JE, Guzzardi M,
574 Decaillet C, Grau M, Dorken B, Lenz P, Lenz G, Thome M. 2011. Malt1-dependent
575 RelB cleavage promotes canonical NF-kappaB activation in lymphocytes and
576 lymphoma cell lines. *Proc Natl Acad Sci U S A* 108:14596-601.
- 577 51. Brustle A, Brenner D, Knobbe CB, Lang PA, Virtanen C, Hershenfield BM, Reardon
578 C, Lacher SM, Ruland J, Ohashi PS, Mak TW. 2012. The NF-kappaB regulator
579 MALT1 determines the encephalitogenic potential of Th17 cells. *J Clin Invest*
580 122:4698-709.
- 581 52. Poeck H, Bscheider M, Gross O, Finger K, Roth S, Rebsamen M, Hanneschlager N,
582 Schlee M, Rothenfusser S, Barchet W, Kato H, Akira S, Inoue S, Endres S, Peschel
583 C, Hartmann G, Hornung V, Ruland J. 2010. Recognition of RNA virus by RIG-I
584 results in activation of CARD9 and inflammasome signaling for interleukin 1 beta
585 production. *Nature Immunology* 11:63-9.
- 586 53. Sghaier I, Zidi S, Mouelhi L, Dabbech R, Ghazouani E, Brochot E, Stayoussef M,
587 Yacoubi-Loueslati B. 2015. The relationship between TNF alpha gene
588 polymorphisms (-238/-308), TNF RII VNTR (p75) and outcomes of hepatitis B virus
589 infection in Tunisian population. *Gene* 568:140-5.
- 590 54. Xu J, Zhang S, Zhang Z, Fu L, Zheng Q, Wang J, Lu S, Du J. 2013. TNF-alpha
591 promoter region polymorphisms affect HBV virus clearance in southern Chinese.
592 *Clin Chim Acta* 425:90-2.
- 593 55. Fletcher NF, Sutaria R, Jo J, Barnes A, Blahova M, Meredith LW, Cosset FL,
594 Curbishley SM, Adams DH, Bertoletti A, McKeating JA. 2014. Activated

- macrophages promote hepatitis C virus entry in a tumor necrosis factor-dependent manner. *Hepatology* 59:1320-30.
56. Park J, Kang W, Ryu SW, Kim WI, Chang DY, Lee DH, Park DY, Choi YH, Choi K, Shin EC, Choi C. 2012. Hepatitis C virus infection enhances TNF α -induced cell death via suppression of NF- κ B. *Hepatology* 56:831-40.
57. Seo SH, Webster RG. 2002. Tumor necrosis factor α exerts powerful anti-influenza virus effects in lung epithelial cells. *J Virol* 76:1071-6.
58. Ebert G, Preston S, Allison C, Cooney J, Toe JG, Stutz MD, Ojaimi S, Scott HW, Baschuk N, Nachbur U, Torresi J, Chin R, Colledge D, Li X, Warner N, Revill P, Bowden S, Silke J, Begley CG, Pellegrini M. 2015. Cellular inhibitor of apoptosis proteins prevent clearance of hepatitis B virus. *Proc Natl Acad Sci U S A* 112:5797-802.
59. Ebert G, Allison C, Preston S, Cooney J, Toe JG, Stutz MD, Ojaimi S, Baschuk N, Nachbur U, Torresi J, Silke J, Begley CG, Pellegrini M. 2015. Eliminating hepatitis B by antagonizing cellular inhibitors of apoptosis. *Proc Natl Acad Sci U S A* 112:5803-8.
60. Beyer M, Abdullah Z, Chemnitz JM, Maisel D, Sander J, Lehmann C, Thabet Y, Shinde PV, Schmidleithner L, Kohne M, Trebicka J, Schierwagen R, Hofmann A, Popov A, Lang KS, Oxenius A, Buch T, Kurts C, Heikenwalder M, Fatkenheuer G, Lang PA, Hartmann P, Knolle PA, Schultze JL. 2016. Tumor-necrosis factor impairs CD4(+) T cell-mediated immunological control in chronic viral infection. *Nature Immunology* 17:593-603.
61. Faber M, Bette M, Preuss MA, Pulmanusahakul R, Rehne J, Schnell MJ, Dietzschold B, Weihe E. 2005. Overexpression of tumor necrosis factor α by a recombinant rabies virus attenuates replication in neurons and prevents lethal infection in mice. *J Virol* 79:15405-16.
62. Junt T, Scandella E, Ludewig B. 2008. Form follows function: lymphoid tissue microarchitecture in antimicrobial immune defence. *Nat Rev Immunol* 8:764-75.
63. Bernhard CA, Ried C, Kochanek S, Brocker T. 2015. CD169+ macrophages are sufficient for priming of CTLs with specificities left out by cross-priming dendritic cells. *Proc Natl Acad Sci U S A* 112:5461-6.
64. Moseman EA, Iannaccone M, Bosurgi L, Tonti E, Chevrier N, Tumanov A, Fu YX, Hacohen N, von Andrian UH. 2012. B cell maintenance of subcapsular sinus macrophages protects against a fatal viral infection independent of adaptive immunity. *Immunity* 36:415-26.
65. Lenardo MJ, Fan CM, Maniatis T, Baltimore D. 1989. The involvement of NF- κ B in beta-interferon gene regulation reveals its role as widely inducible mediator of signal transduction. *Cell* 57:287-94.
66. Hiscott J, Alper D, Cohen L, Leblanc JF, Sportza L, Wong A, Xanthoudakis S. 1989. Induction of human interferon gene expression is associated with a nuclear factor that interacts with the NF- κ B site of the human immunodeficiency virus enhancer. *J Virol* 63:2557-66.
67. Wang X, Hussain S, Wang EJ, Li MO, Garcia-Sastre A, Beg AA. 2007. Lack of essential role of NF- κ B p50, RelA, and cRel subunits in virus-induced type 1 IFN expression. *J Immunol* 178:6770-6.

- 640 68. Wang J, Basagoudanavar SH, Wang X, Hopewell E, Albrecht R, Garcia-Sastre A,
641 Balachandran S, Beg AA. 2010. NF-kappa B RelA subunit is crucial for early IFN-
642 beta expression and resistance to RNA virus replication. *J Immunol* 185:1720-9.
- 643 69. Wang X, Wang J, Zheng H, Xie M, Hopewell EL, Albrecht RA, Nogusa S, Garcia-
644 Sastre A, Balachandran S, Beg AA. 2014. Differential requirement for the
645 IKKbeta/NF-kappaB signaling module in regulating TLR- versus RLR-induced type
646 1 IFN expression in dendritic cells. *J Immunol* 193:2538-45.
- 647 70. Jin J, Hu H, Li HS, Yu J, Xiao Y, Brittain GC, Zou Q, Cheng X, Mallette FA,
648 Watowich SS, Sun SC. 2014. Noncanonical NF-kappaB pathway controls the
649 production of type I interferons in antiviral innate immunity. *Immunity* 40:342-54.
- 650 71. Ruland J, Duncan GS, Wakeham A, Mak TW. 2003. Differential requirement for
651 Malt1 in T and B cell antigen receptor signaling. *Immunity* 19:749-58.
- 652 72. Oetke C, Vinson MC, Jones C, Crocker PR. 2006. Sialoadhesin-deficient mice exhibit
653 subtle changes in B- and T-cell populations and reduced immunoglobulin M levels.
654 *Mol Cell Biol* 26:1549-57.
- 655 73. Jung S, Unutmaz D, Wong P, Sano G, De los Santos K, Sparwasser T, Wu S,
656 Vuthoori S, Ko K, Zavala F, Pamer EG, Littman DR, Lang RA. 2002. In vivo
657 depletion of CD11c+ dendritic cells abrogates priming of CD8+ T cells by exogenous
658 cell-associated antigens. *Immunity* 17:211-20.
- 659 74. Miyake Y, Asano K, Kaise H, Uemura M, Nakayama M, Tanaka M. 2007. Critical
660 role of macrophages in the marginal zone in the suppression of immune responses to
661 apoptotic cell-associated antigens. *J Clin Invest* 117:2268-78.
- 662 75. Iwata A, Nishio K, Winn RK, Chi EY, Henderson WR, Jr., Harlan JM. 2003. A
663 broad-spectrum caspase inhibitor attenuates allergic airway inflammation in murine
664 asthma model. *J Immunol* 170:3386-91.
- 665 76. Hotchkiss RS, Chang KC, Swanson PE, Tinsley KW, Hui JJ, Klender P,
666 Xanthoudakis S, Roy S, Black C, Grimm E, Aspiotis R, Han Y, Nicholson DW, Karl
667 IE. 2000. Caspase inhibitors improve survival in sepsis: a critical role of the
668 lymphocyte. *Nature Immunology* 1:496-501.
- 669
- 670
- 671
- 672
- 673

674 **Figure Legends**

675 **Fig. 1: Vesicular stomatitis virus infection leads to infiltration of TNF producing**
676 **phagocytes.**

677 **(A to F)** WT mice were infected with 2×10^8 PFU vesicular stomatitis virus (VSV). **(A)**
678 Tumor necrosis factor (TNF)- α mRNA expression levels in WT spleen tissue were
679 determined at the indicated time points after infection ($n=4-10$). **(B)** Surface molecule
680 expression of CD11b, CD11c, CD8, and CD19 on TNF $^{+}$ cells is shown 4h after infection
681 (purple gate, whole spleen; pink gate, TNF $^{+}$ cells) (one representative result of $n=5$ is shown).
682 **(C)** Splenocytes from WT mice were stained for intracellular TNF production. TNF $^{+}$ CD11b $^{+}$
683 cells were determined (as % of total CD11b $^{+}$ cells; $n=5$). **(D)** TNF- α mRNA expression was
684 determined in the spleen of WT, *Jh* $^{-/-}$, *Rag* $^{-/-}$, and *CD8* $^{-/-}$ mice 4 h after infection ($n=5-6$). **(E)**
685 Surface molecule expression of TNF producing cells is shown 4h after infection. CD3 $^{-}$ CD8 $^{-}$
686 CD19 $^{-}$ NK1.1 $^{-}$ cells were further characterized for expression of CD11b, CD11c, Ly6C,
687 Ly6G, F4/80, MHC II, and CD115 on TNF $^{+}$ cells ($n=6$). **(F)** CD3 $^{-}$ CD8 $^{-}$ CD19 $^{-}$ NK1.1 $^{-}$
688 CD11b $^{+}$ Ly6C $^{+}$ Ly6G $^{+}$ TNF $^{+}$ cells were quantified in spleen tissue 4h after infection ($n=6$).
689 **(G)** Mice were injected with PBS-liposomes or clodronate- liposomes. Spleen tissue was
690 harvested after 24h. Sections from snap frozen spleen tissue were stained with anti-F4/80
691 antibodies ($n=3$). **(H)** TNF- α mRNA expression was determined in the spleen of WT,
692 clodronate-treated WT, *Ifnar* $^{-/-}$, DT-treated CD169-DTR, and CD11c-DTR mice 4 h after
693 infection ($n=6$).

694

695 **Fig. 2: Tumor necrosis factor is required for early innate immune activation via**
696 **maintenance of CD169⁺ cells during viral infection.**

697 **(A to D)** Mice were infected with 10^5 PFU VSV. **(A)** Survival of Wild-type (WT) and tumor
698 necrosis factor- α null (*Tnfa*^{-/-}) mice was monitored for 20 days after infection ($n=9-12$). **(B)**
699 Titers of neutralizing total immunoglobulin (Ig; left) and IgG (right) were determined in WT
700 and *Tnfa*^{-/-} mice at indicated time points after infection ($n=7$). **(C)** Interferon (IFN)- α and β
701 concentrations were determined in the sera of WT and *Tnfa*^{-/-} mice 24 h after infection ($n=6-9$). **(D)** IFN- α levels were determined in sera from WT and CD169-DTR mice 24 h after
702 infection ($n=6$). **(E)** IFN- α and β concentration was determined in the sera of WT and *Tnfa*^{-/-}
703 mice injected with 200 μ g of polyinosinic:polycytidylic acid (polyI:C) at indicated time
704 points ($n=3$). **(F)** WT and *Tnfa*^{-/-} mice were infected with 2×10^8 plaque-forming units
705 (PFU) of VSV. Snap-frozen spleen sections were stained with anti-CD169 antibodies (clone:
706 MOMA-1) at indicated time points (one representative result of $n=6$ mice is shown; scale bar
707 = 100 μ m). **(G)** MFI of CD169 was quantified across spleen section from naïve and VSV
708 infected WT and *Tnfa*^{-/-} mice using ImageJ (1-3 images per spleen from 3-4 mice were
709 analyzed). **(H)** MFI from *Tnfa*^{-/-} mice was normalized to WT MFI **(I)** Snap-frozen spleen
710 sections from WT and *Tnfa*^{-/-} mice were stained for VSV glycoprotein (VSV-G) expression
711 (clone: Vi10) after infection with 2×10^8 PFU VSV at indicated time points (one
712 representative result of $n=6$ mice is shown; scale bar = 100 μ m). **(J)** MFI of VSV-G
713 expression was quantified across spleen section from naïve and VSV infected WT and *Tnfa*^{-/-}
714 mice using ImageJ (1-3 images per spleen from 3-4 mice were analyzed) **(K)** WT and *Tnfa*^{-/-}
715 mice were infected with 10^5 PFU VSV. Viral titers were measured in the spleen of WT and
716 *Tnfa*^{-/-} mice 8 h after infection with VSV ($n=6$). **(L)** *Tnfa* mRNA expression was determined

718 in spleen tissue of WT mice before and 4h after injection with UV-inactivated VSV ($n=4$).
719 (M) Spleen tissue sections were stained with anti-CD169 antibodies in WT and *Tnfa*^{-/-} mice
720 8h after infection with 2×10^8 PFU of ultraviolet (UV)-inactivated VSV (one representative
721 result of $n=3$ is shown). (N) Sections from snap-frozen spleen tissue harvested from WT and
722 *CD169*^{-/-} mice were stained for CD169 and VSV-G 7h after infection with 2×10^8 PFU VSV
723 ($n=3$; scale bar = 100 μ m).

724

725 **Fig. 3: VSV replication is sustained via TNFR1 on CD169⁺ cells.**

726 (A) Spleen tissue sections from wild-type (WT), *Tnfrsf1a*^{-/-} (tumor necrosis factor receptor 1
727 [TNFR1]), and *Tnfrsf1b*^{-/-} (TNFR2) mice were stained with anti-CD169 and VSV-G
728 antibodies 8 h after infection with 2×10^8 PFU of VSV (One representative result of $n=6$
729 mice is shown; scale bar = 100 μ m). (B) MFI of CD169 was quantified across spleen sections
730 from WT, *Tnfrsf1a*^{-/-}, and *Tnfrsf1b*^{-/-} infected mice, using ImageJ (1-3 images per spleen from
731 3-4 mice were analyzed). (C-G) WT, *Tnfrsf1a*^{-/-}, and *Tnfrsf1b*^{-/-} mice were infected with 10^5
732 PFU VSV. (C) Viral titers were measured in spleen tissue 8h after infection in WT, *Tnfrsf1a*^{-/-}
733 ^{-/-}, and *Tnfrsf1b*^{-/-} mice ($n=6-9$). (D) IFN- α concentration was determined in the sera of WT,
734 *Tnfrsf1a*^{-/-}, and *Tnfrsf1b*^{-/-} mice 24 h after infection with VSV ($n=6-9$). (E) WT and *Tnfrsf1a*^{-/-}
735 ^{-/-} mice were infected with 10^5 PFU VSV. RNA expression levels of indicated genes were
736 determined in brain and spinal cord 24 h after infection ($n=4-7$, highest relative expression
737 values brain/spinal cord: *Eif2ak2*, 13.72/7.98; *Ifit2*, 5.41/6.13; *Ifit3*, 35.99/34.15; *Irf7*,
738 68.80/54.55; *Isg15*, 42.54/51.23; *Oasl1*, 70.43/84.94). (F) WT and *Tnfrsf1b*^{-/-} mice were
739 infected with 10^5 PFU VSV. RNA expression levels of indicated genes were determined in

740 brain and spinal cord 24h after infection (n=3-4, highest relative expression values
741 brain/spinal cord: *Eif2ak*, 29.84/18.21; *Ifit2*, 7.99/10.24; *Ifit3*, 41.05/51.25; *Irf7*,
742 166.79/88.58; *Isg15*, 29.78/52.99; *Oas1l*, 75.60/114.39). (G) Viral titers were measured in
743 brain and spinal cord tissue of WT and *Tnfrsf1a*^{-/-} mice, once *Tnfrsf1a*^{-/-} mice exhibited hind
744 limb paralysis (n=3). (H) Survival of WT, *Tnfrsf1a*^{-/-}, and *Tnfrsf1b*^{-/-} mice was monitored
745 over time after infection with VSV (n=15-24).

746

747 **Fig. 4: TNFR1 on CD169⁺ cells is essential for early IFN-I response.**

748 (A) Follicular B cells (CD19⁺CD23⁺) (FB), marginal zone B cells (CD19⁺CD21⁺ CD23⁻)
749 (MZB), and regulatory B cells (CD19⁺CD21⁺ CD5⁺IgM⁺) (RB) were analyzed in naïve WT,
750 *Tnfa*^{-/-}, *Tnfrsf1a*^{-/-}, and *Tnfrsf1b*^{-/-} deficient mice (n=6). (B) Lymphotoxin α (*LT α*), *LT β* , and
751 lymphotoxin β receptor (*Lt β R*) gene expression was determined in spleen tissue from WT
752 and *Tnfrsf1a*^{-/-} mice by reverse-transcription polymerase chain reaction (RT-PCR) (n=3). (C)
753 Splenic B-cell populations FB, MZB, and RB were analyzed after infection with 2 \times 10⁸ PFU
754 of VSV in WT and *Tnfrsf1a*^{-/-} mice at indicated time points (n=5). (D) IFN- α concentration
755 was determined 24 h after infection with 10⁵ PFU VSV in the sera of lethally irradiated mice
756 reconstituted with either WT:*Rag*^{-/-} or *Tnfrsf1a*^{-/-}:*Rag*^{-/-} bone marrow at a ratio of 1:1 (n=4).
757 (E) Neutralizing total immunoglobulin (Ig; left) and IgG (right) antibody titers were
758 determined in the sera of WT:*Rag*^{-/-} or *Tnfrsf1a*^{-/-}:*Rag*^{-/-} reconstituted animals (n=4). (F-H)
759 Lethally irradiated WT mice were reconstituted with bone marrow (BM) from WT or
760 *Tnfrsf1a*^{-/-} mice mixed with BM from (F) CD169-DTR and (H) CD11c-DTR at a 1:1 ratio.
761 After 40 days, mice were infected with 10⁵ PFU of VSV. Before the infection mice were

762 treated with 2 doses of 100 ng DT via intra peritoneal injection (**F**) IFN- α concentration was
763 determined 24h after infection in the sera of WT:CD169-DTR and *Tnfrsf1a*^{-/-}:CD169-DTR
764 reconstituted animals ($n=4-5$). (**G**) Neutralizing total immunoglobulin (Ig; left) and IgG
765 (right) antibody titers were determined in the sera of WT:CD169-DTR and *Tnfrsf1a*^{-/-}
766 :CD169-DTR reconstituted animals after infection with 10^5 PFU VSV at indicated time
767 points ($n=4$). (**H**) IFN- α concentration was determined 24 h after infection in the sera of
768 WT:CD11c-DTR and *Tnfrsf1a*^{-/-}:CD11c-DTR reconstituted mice ($n=4-5$).

769

770 **Fig. 5: Tumor necrosis factor mediates survival of CD169⁺ cells via TNFR1**

771 (**A-E**) Mice were infected with 2×10^8 PFU VSV. (**A**) Caspase 3 activity was determined in
772 spleen tissue harvested from WT and *Tnfa*^{-/-} mice 6h after infection with 2×10^8 PFU VSV
773 ($n=4-7$, RFU = relative fluorescence units). (**B**) *Bcl2*, *Bclxl*, *Xiap* RNA expression was
774 determined in spleen tissue from WT and *Tnfrsf1a*^{-/-} mice 8h after infection ($n=3$). (**C**)
775 Tissue sections from WT and *Tnfa*^{-/-} mice were stained with terminal deoxynucleotidyl
776 transferase dUTP nick end labeling (TUNEL) 5 h after infection (one result representative of
777 3 or 4 mice is shown; scale bar = 10 μ m). (**D**) Mean fluorescence intensity (MFI) of TUNEL
778 was quantified across spleen sections from naïve and VSV infected WT and *Tnfa*^{-/-} mice
779 using ImageJ (1-2 images per spleen from 3-4 mice were analyzed). (**E**) At indicated time
780 points, the proportion of 7 aminoactinomycin D-positive (7AAD⁺) cells among
781 CD11b⁺CD169⁺ cells were determined ($n=5$) in WT and *Tnfrsf1a*^{-/-} mice. (**F**) WT, *Tnfa*^{-/-} and
782 *Tnfrsf1a*^{-/-} mice were treated with Z-Val-Ala-Asp-fluoromethylketone (zVAD-FMK) and
783 infected with 2×10^8 PFU VSV. Spleen tissue sections were stained with anti-CD169

antibodies 8 h after infection (one result representative of 3-4 mice is shown; scale bar = 100 μ m). (G) MFI of CD169 was quantified across spleen sections from naïve and VSV infected WT and *Tnfa*^{-/-} mice treated with Z-VAD using ImageJ (1-3 images per spleen from 3-4 mice were analyzed). (H) IFN- α concentration was determined 24 h after infection in the sera of Z-VAD treated WT and *Tnfa*^{-/-} mice after infection with 10⁵ PFU of VSV (n=3).

789

Fig. 6: VSV infection leads to TNFR1 dependent canonical NF- κ B activation in splenic CD169⁺ cells.

(A-D) Sections of snap-frozen spleen tissue were harvested 4h after infection with 2 x 10⁸ PFU VSV. (A) Sections were stained for RelA before and after infection (one representative result of n=3 is shown; scale bar = 100 μ m; side panel shows a cropped image; scale bar = 5 μ m). (B) MFI of cytoplasmic and respective nuclear RelA was quantified in CD169⁺ cells from WT mice before and after VSV infection to evaluate nuclear translocation of RelA (n = 48-63 are shown). (C to E) Spleen sections from WT and (C) *Tnfa*^{-/-}, (D) *Tnfrsf1a*^{-/-} and (E) *Tnfrsf1b*^{-/-} mice were stained with anti-RelA antibodies 4h after infection with 2x10⁸ PFU VSV. MFI of RelA in the nucleus of CD169⁺ was determined with ImageJ software (n=35-57).

801

Fig. 7: MALT1 regulates translocation of RelA into the nucleus after infection with vesicular stomatitis virus.

803

804 (A) Sections from snap-frozen spleen tissue harvested from naive *Malt1*^{+/-} and *Malt1*^{-/-} mice
805 were stained with anti-RelB antibodies (one representative result of n=3 is shown; scale bar =
806 10 μ m). (B) MFI of cytoplasmic and nuclear RelB was quantified in CD169⁺ cells using
807 ImageJ (n=39-42). (C) Sections of snap-frozen spleen tissue from *Malt1*^{+/-} and *Malt1*^{-/-} mice
808 were stained with anti-RelA antibodies 4h after infection with 2 x 10⁸ PFU VSV. The MFI in
809 the nucleus of CD169⁺ cells was quantified (n=29-41). (D+E) *Malt1*^{+/-} and *Malt1*^{-/-} mouse
810 embryonic fibroblasts (MEFs) were stimulated with 100 ng/ml recombinant mouse tumor
811 necrosis factor (rmTNF) at indicated time points. Cytosolic (CE) and nuclear extracts (NE)
812 were harvested and probed for p65. Densitometry analysis of p65 and RelB was performed
813 on the WB images from cytosolic and nuclear fractions at indicated time points. Proteins
814 were normalized to GAPDH or histone (n=4).

815 **Fig. 8: MALT1 promotes vesicular stomatitis virus replication in CD169⁺ cells and**
816 **immune activation during viral infection.**

817 (A) Spleen sections from naïve *Malt1*^{+/-} and *Malt1*^{-/-} mice were stained with anti-CD169 (one
818 representative result of n=3 is shown; scale bar = 100 μ m). (B) Sections of snap-frozen
819 spleen tissue from *Malt1*^{+/-} and *Malt1*^{-/-} mice were analyzed 8h after infection with 2 x 10⁸
820 PFU VSV, stained with anti-CD169 and anti-vesicular stomatitis virus glycoprotein (VSV-
821 G) (one representative result of n=3 is shown; scale bar = 100 μ m). (C) MFI of CD169 and
822 VSV-G was quantified across spleen sections from VSV infected *Malt1*^{+/-} and *Malt1*^{-/-} mice
823 using ImageJ (n=4). (D and E) Mice were infected with 10⁵ PFU VSV. (D) Viral titers were
824 measured in spleen tissue of *Malt1*^{+/-} and *Malt1*^{-/-} mice 8h after infection (n=6). (E) IFN- α
825 concentration was determined in the sera of *Malt1*^{+/-} and *Malt1*^{-/-} mice 24 h after infection
826 (n=6). (F) IFN- α concentration was determined in the sera of *Malt1*^{+/-} and *Malt1*^{-/-} mice

827 injected with 200µg polyinosinic:polycytidylic acid (poly I:C) at indicated time points ($n=3$ -
828 4). (G) Survival of *Malt1*^{+/-} and *Malt1*^{-/-} animals was monitored for 20 days after infection
829 ($n=13-14$).

Fig. 1

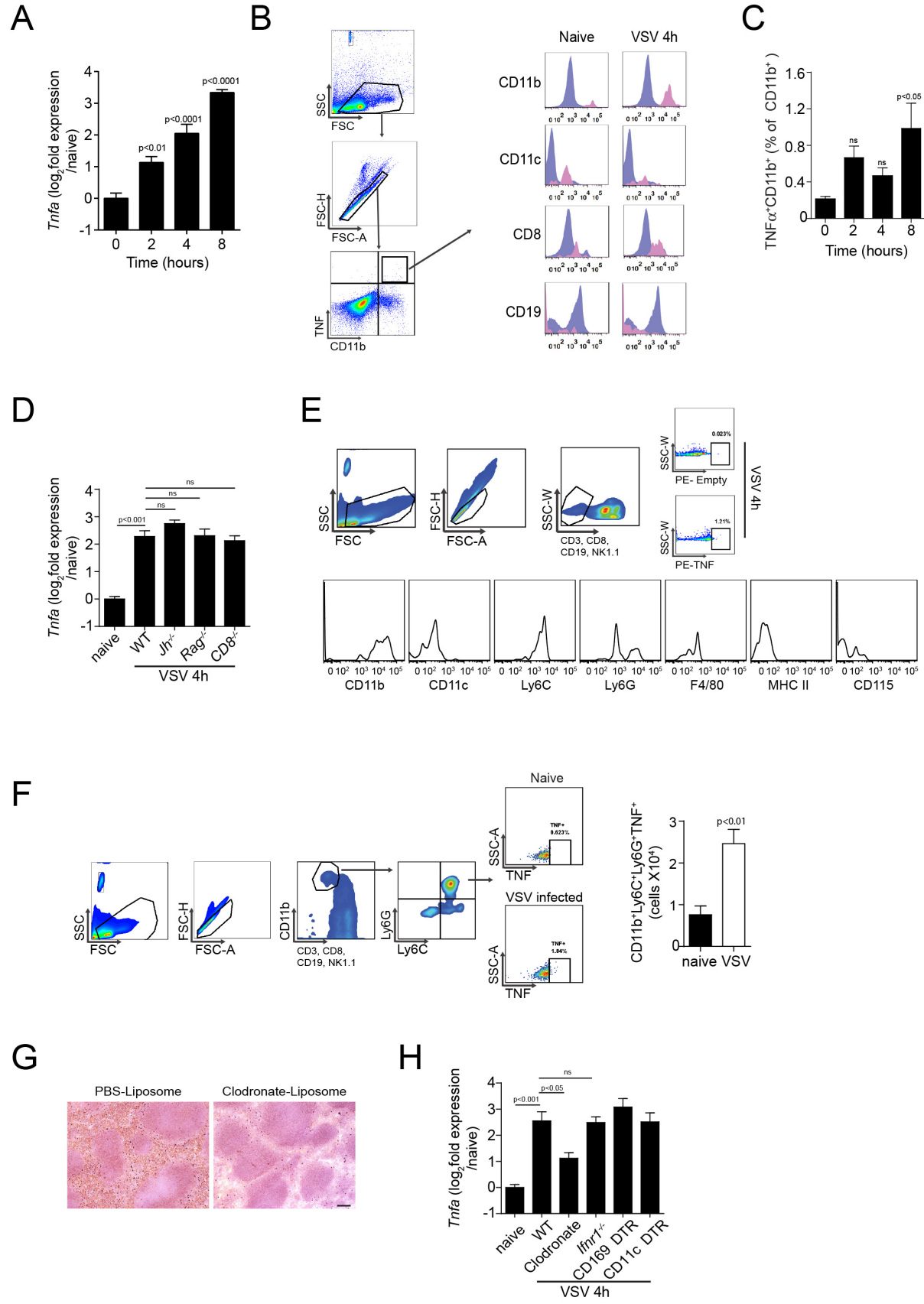


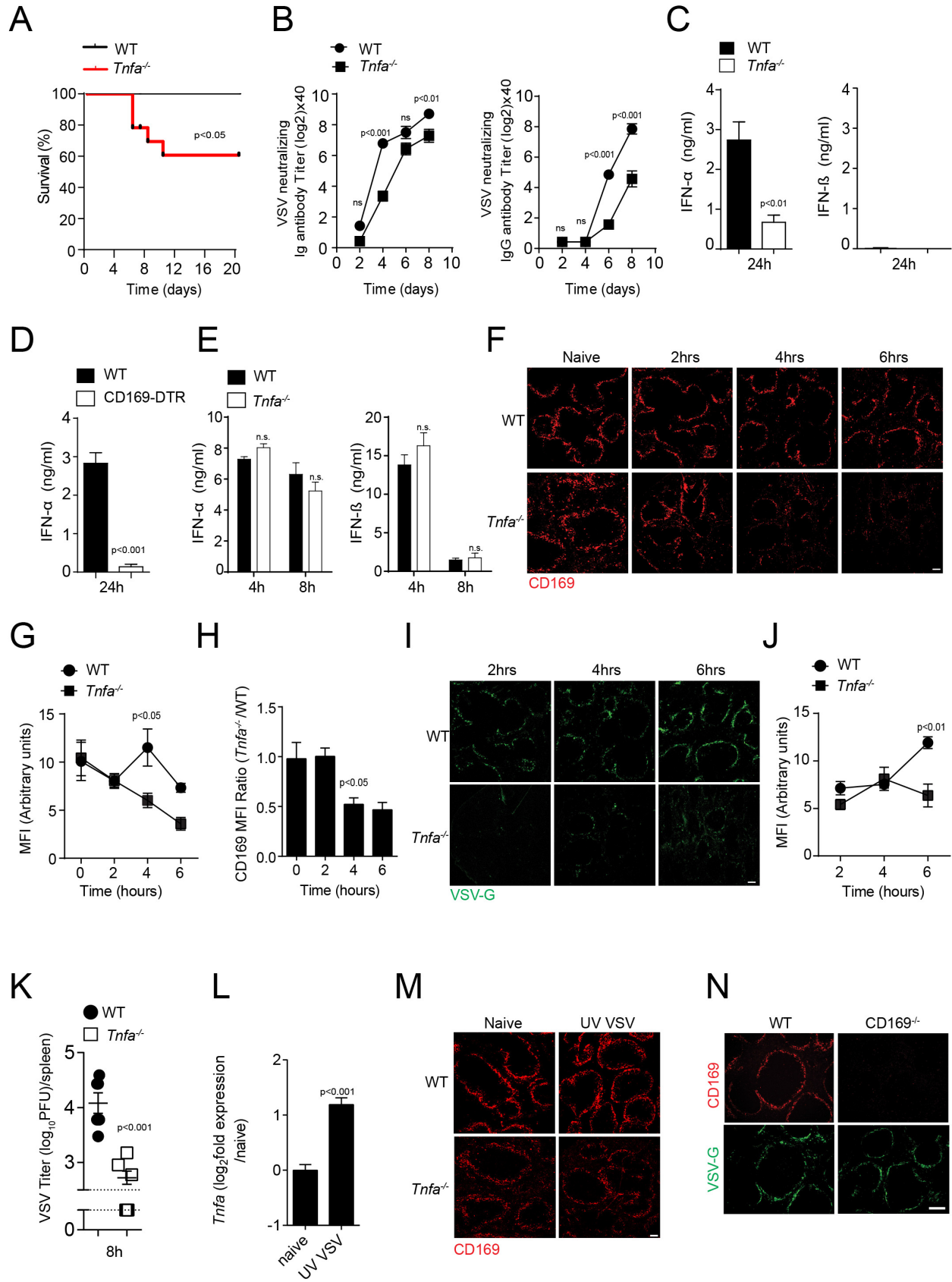
Fig. 2

Fig. 3

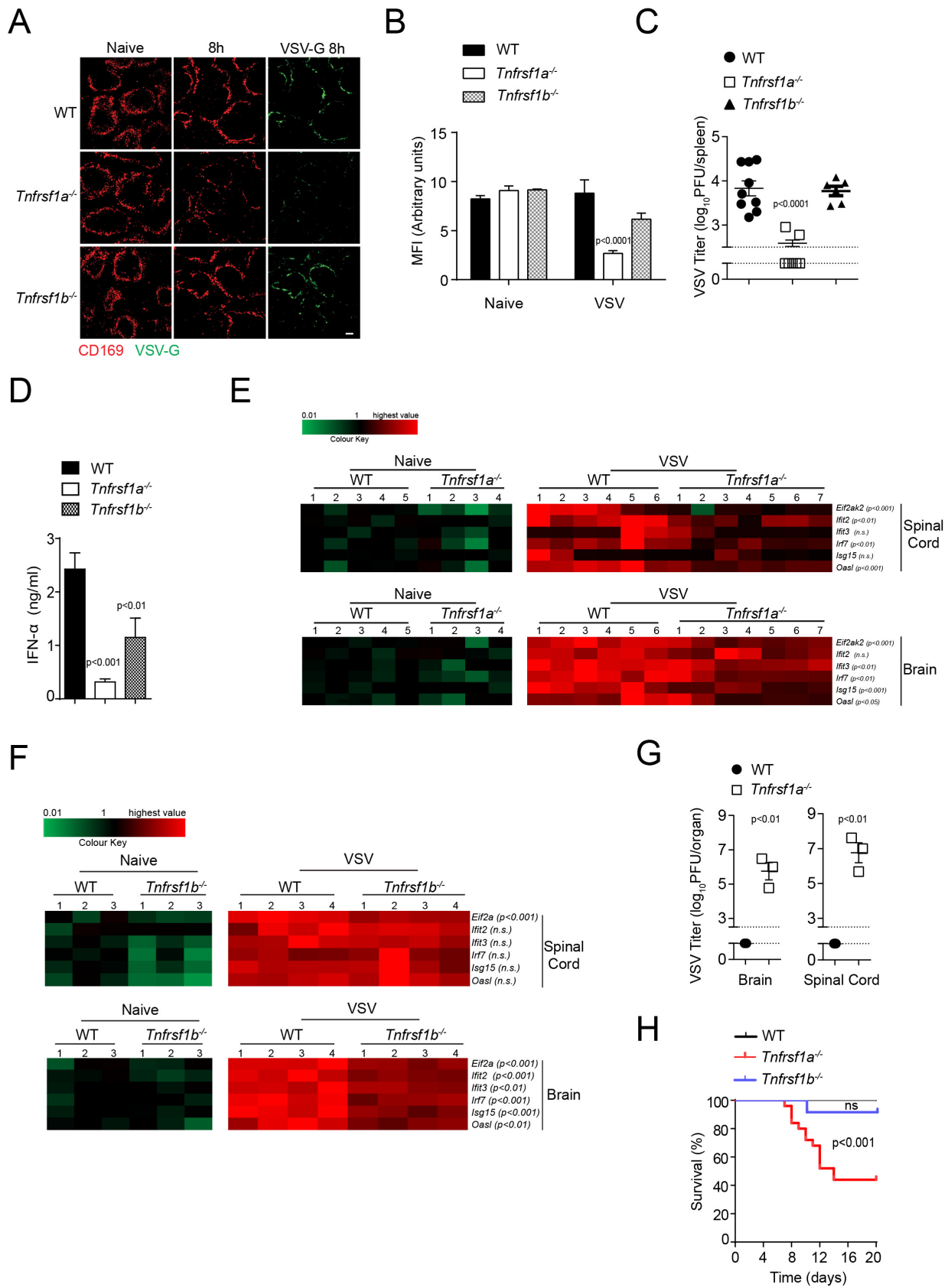


Fig 4

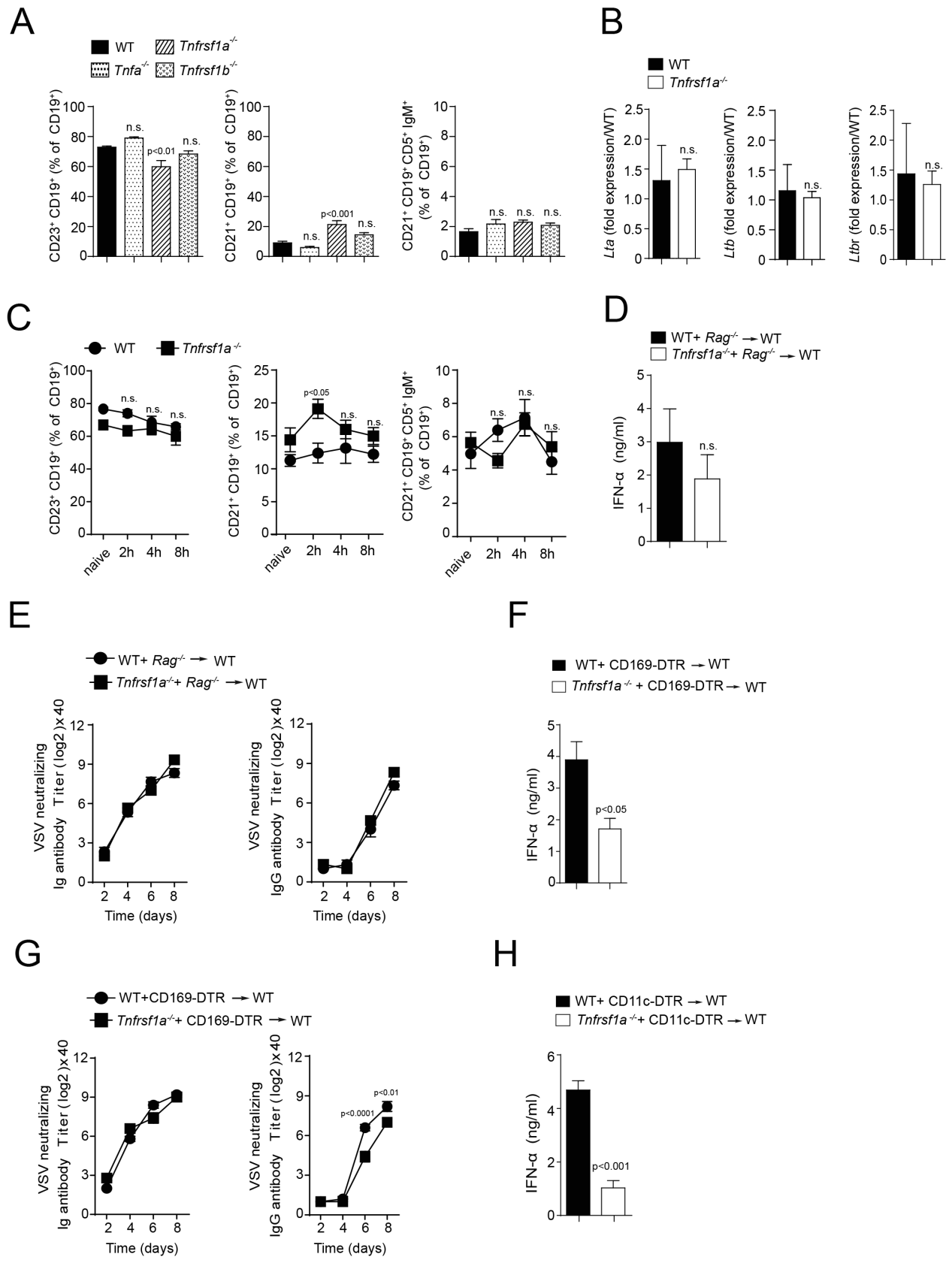


Fig.5

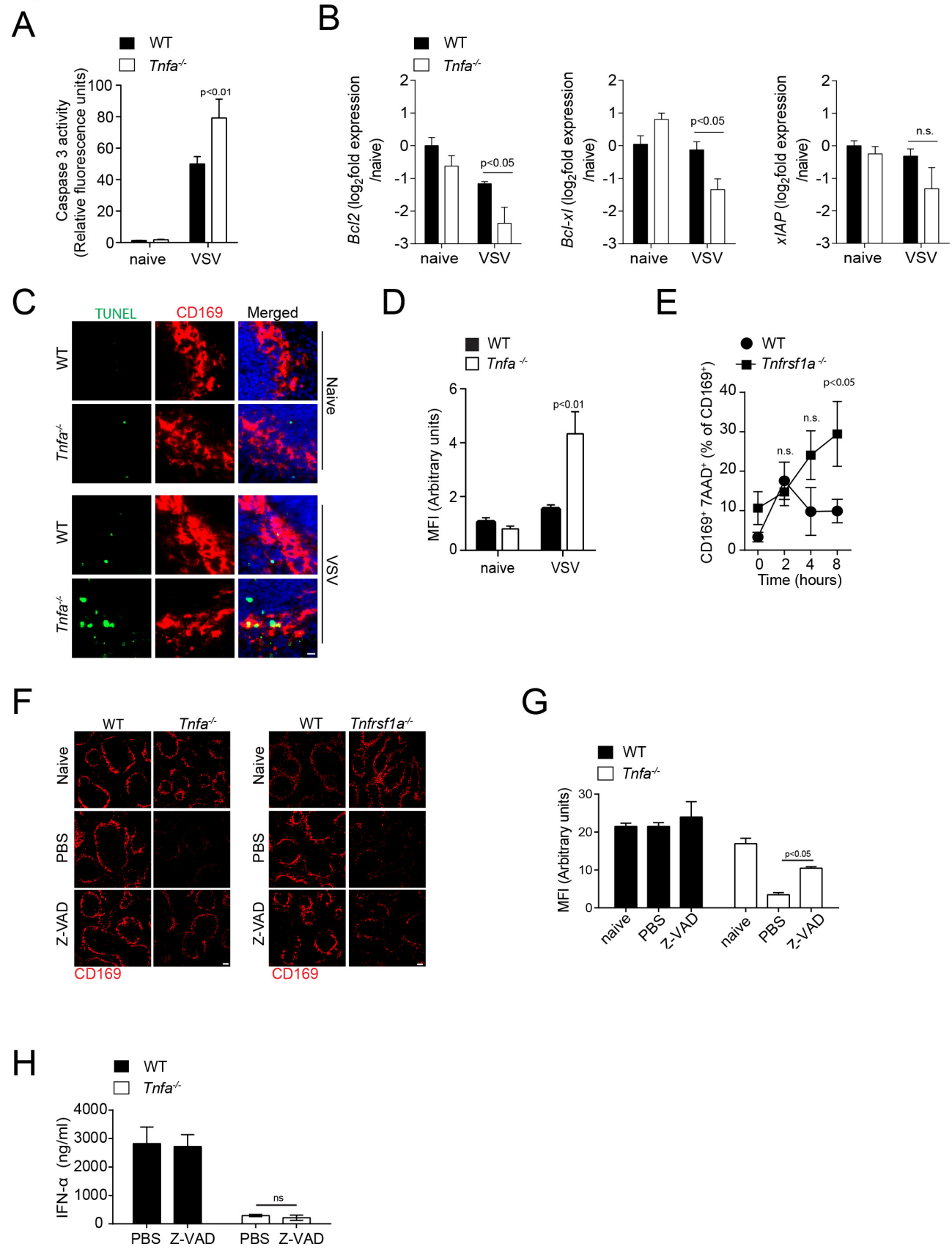


Fig. 6

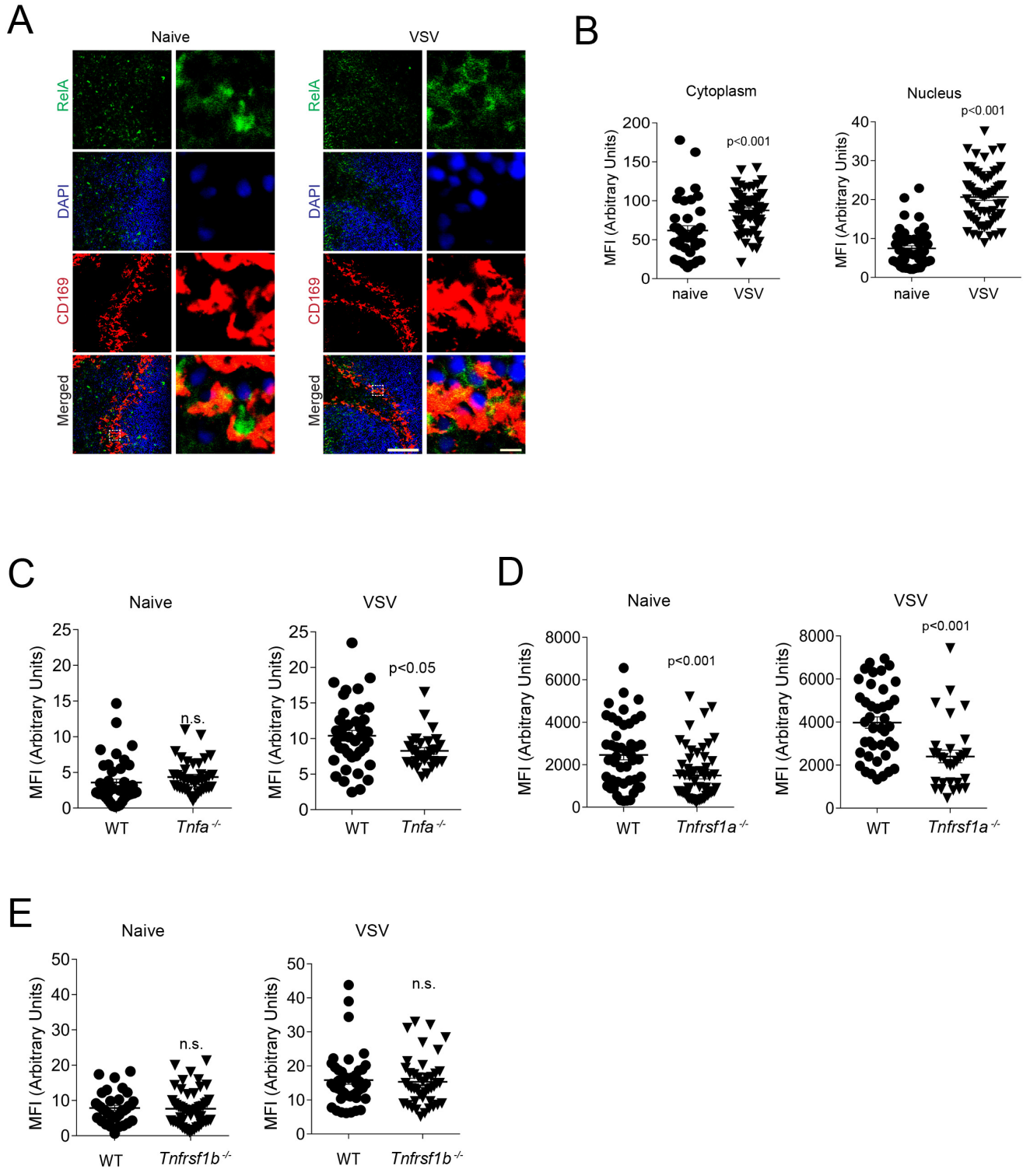
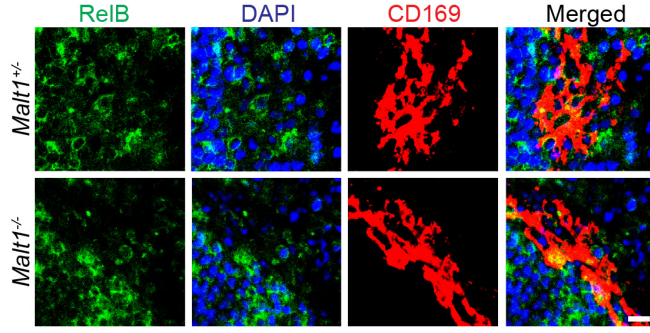
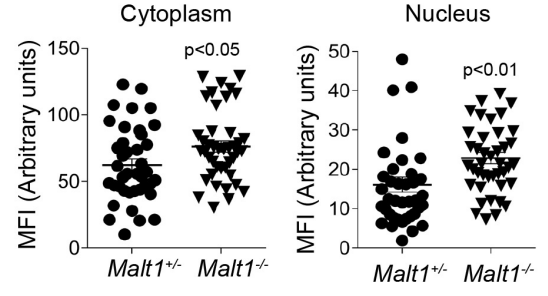


Fig. 7

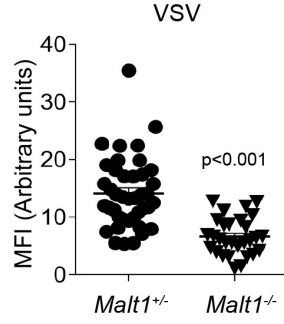
A



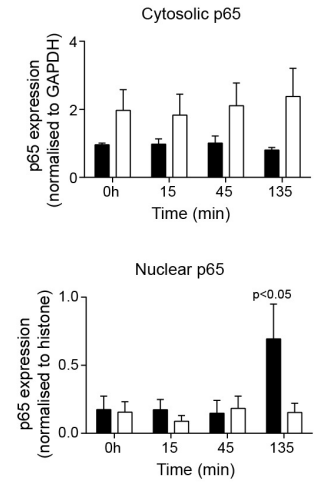
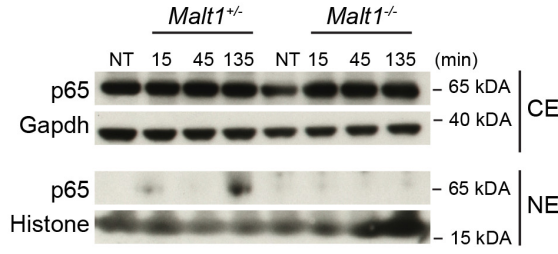
B



C



D



E

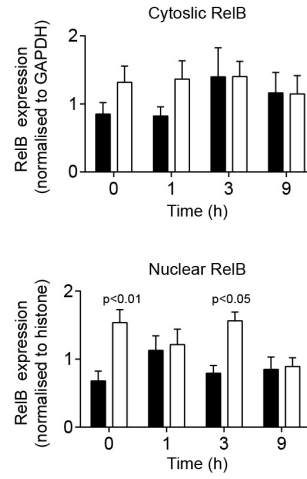
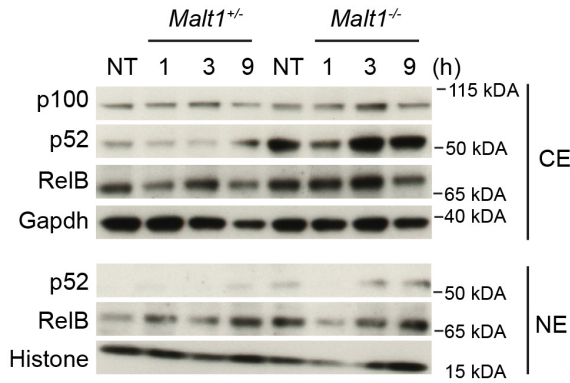


Fig. 8

